

## Electronic Supplementary Information

# A new octa-Mn-substituted poly(polyoxotungstate)

Hai-Lou Li, Chen Lian, Da-Peng Yin and Guo-Yu Yang\*

MOE Key Laboratory of Cluster Science, School of Chemistry and Chemical Engineering, Beijing Institute of Technology, Beijing 102488, China. E-mail: ygy@bit.edu.cn

**Figure S1.** The experimental and simulated PXRD patterns of **1**.

**Figure S2.** The polyoxoanion of **1**. Atoms with A in their labels are symmetrically generated. A: x, -1-y, z.

**Figure S3.** The hexagon of six W/Mn atoms. Atoms with A in their labels are symmetrically generated. A: x, -1-y, z.

**Figure S4.** (a), (b) The 1-D chain packing view and the simplified packing of **1**, along the *a*-axis.

**Figure S5.** The TG curve of **1**.

**Figure S6.** The IR spectrum of **1**

**Figure S7.** The IR spectra of **1** at different temperatures.

**Figure S8.** Field dependence of the magnetization of **1**.

**Table S1.** Bond valence sum (BVS) calculations of some W, Mn, and Si atoms in **1**

### Materials and physical measurements

The precursor of  $\text{Na}_{10}[\text{A}-\alpha\text{-SiW}_9\text{O}_{34}]\cdot18\text{H}_2\text{O}$  was synthesized as previously described<sup>1</sup> and further identified by IR spectroscopy. All other chemicals are commercially purchased without further purification and disposal. Carbon and hydrogen elemental analysis were performed on a Perkin–Elmer 2400-II CHNS / O analyzer. IR spectra were recorded with a Smart Omni-Transmission spectrometer using KBr pellets in the range of 400–4000  $\text{cm}^{-1}$ . Powder X-ray diffraction (PXRD) pattern was obtained by using a Bruker D8 Advance XRD diffractometer with  $\text{Cu K}\alpha$  radiation ( $\lambda = 1.54056 \text{ \AA}$ ). Thermogravimetric (TG) analysis was performed under a  $\text{N}_2$  atmosphere on a Mettler–Toledo TGA/SDTA 851e instrument with a heating rate of  $10 \text{ }^{\circ}\text{C min}^{-1}$  from 25 to  $500 \text{ }^{\circ}\text{C}$ . Cyclic voltammograms (CV) were recorded on a CS electrochemical workstation at room temperature. In throughout the experiments, we used twice-distilled water, a three-electrode system and a carbon paste electrode acted as a working electrode, the counter electrode was a platinum gauze, an Ag/AgCl electrode was used as a referenced. The supporting electrolyte of **1** was  $\text{Na}_2\text{SO}_4 + \text{H}_2\text{SO}_4$  aqueous solution ( $0.5 \text{ mol L}^{-1}$ ). Magnetic property was investigated on a Quantum Design SQUID MPMS3 magnetometer.

<sup>1</sup> G. Hervé and A. Tézé, *Inorg. Chem.*, 1977, **16**, 2115.

### X-ray crystallography

A suitable crystal of **1** was selected from the mother liquor and mounted on fiber glass and then transferred directly to a Bruker APEX-II CCD detector at 296(2) K with Mo K $\alpha$  monochromated radiation ( $\lambda = 0.71073 \text{ \AA}$ ). The structure was solved by the direct method and refined on  $F^2$  by full-matrix least-squares methods using the SHELX-2016/6 program package.<sup>1</sup> No hydrogen atoms associated with water molecules were located from the difference Fourier map. In the structural refinements, the “omit” constraint was used owing to the low-quality diffraction data in high  $\theta$ , the contribution of these disordered solvent molecules to the overall intensity data of all structures was treated using the SQUEEZE method in PLATON. In order to balance the charge of compound **1**, 19 protons should be added. These protons cannot be located crystallographically and are assumed to be delocalized over the entire structure, which is very common in POMs.<sup>2</sup> In the refinements, 3 dimethylamine molecules for **1** are found from the Fourier maps. In addition, on the basis of elemental analysis and TGA, 5 dimethylamine molecules for **1** are directly added to molecular formula. The crystallographic data and structure refinement parameters for **1** are listed in Table 1.

1 (a) G.M. Sheldrick, *Acta. Crystallogr. Sect. C.*; 2015, **71**, 3; (b) G. M. Sheldrick, SHELXS, 2016/6 Program for Crystal Structure Solution, University of Göttingen, 2016.

2 (a) F. Bannani, S. Floquet, N. Leclerc-Laronze, M. Haouas, F. Taulelle, J. Marrot, P. Köerler and E. Cadot, *J. Am. Chem. Soc.*, 2012, **134**, 19342; (b) H.-L. Li, Z. Zhang, Y.-L. Wang and G.-Y. Yang, *Eur. J. Inorg. Chem.*, 2019, 486.

### Thermogravimetric analysis (TGA)

To study the thermal stability and determine the number of lattice water molecules and free organic molecules of **1**, the TG curve was measured in the temperature range of 25–500°C under flowing N<sub>2</sub> atmosphere. It is easy to see from Figure S5 that the weight loss of compound **1** is a two-step process. Primarily, the first step weight loss of 4.87 % (calcd. 4.78%) takes place between 25 and 200°C attributed to the loss of thirty-one lattice water molecules. The second step weight loss of 5.22% (calcd. 5.17 %) occurs at 200 - 500 °C due to the removal of eight dimethylamine groups and the dehydration of twenty-seven protons. The overall weight loss is 10.09% (calcd. 9.95%) for **1**. Obviously, the TG result is basically consistent with the structural determination.

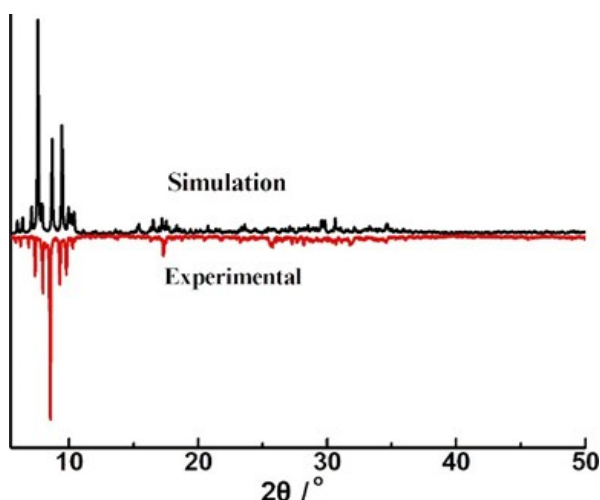


**Figure S1.** The experimental and simulated PXRD patterns of **1**.

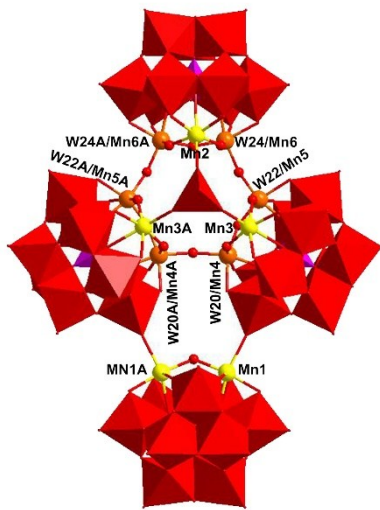


**Figure S2.** The polyoxoanion of **1**. Atoms with A in their labels are symmetrically generated. A:  $x, -1-y, z$ .

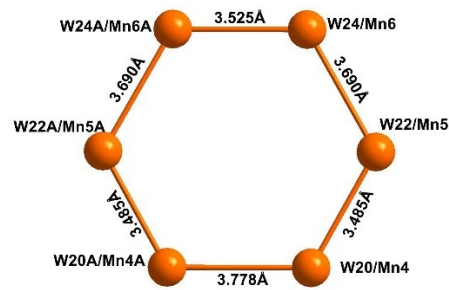


**Figure S3.** The hexagon of six W/Mn atoms. Atoms with A in their labels are symmetrically generated. A:  $x, -1-y, z$ .

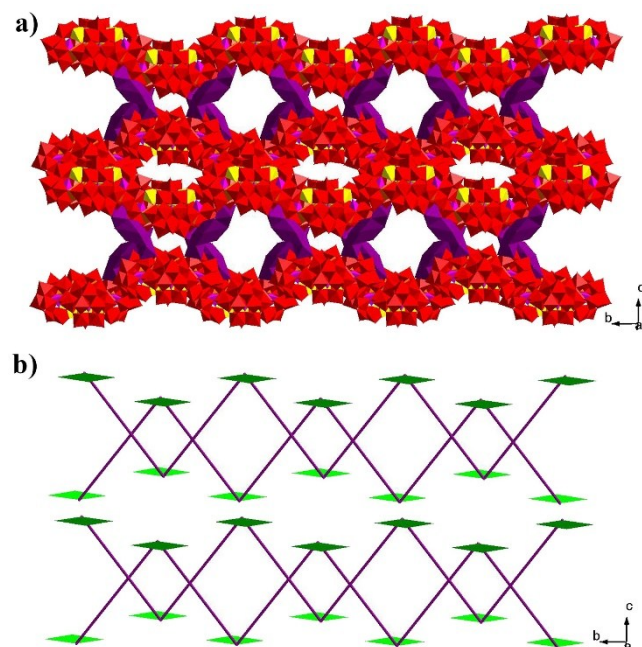


**Figure S4.** (a), (b) The 1-D chain packing view and the simplified packing of **1**, along the  $a$ -axis.

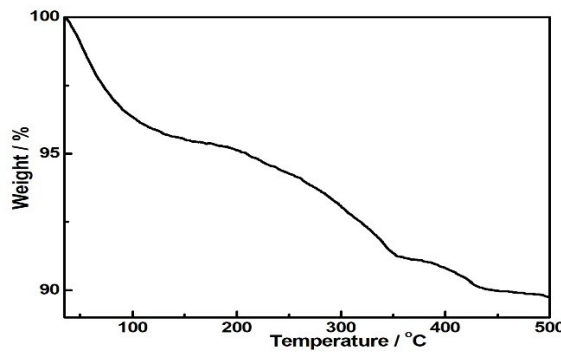


**Figure S5.** The TG curve of **1**.

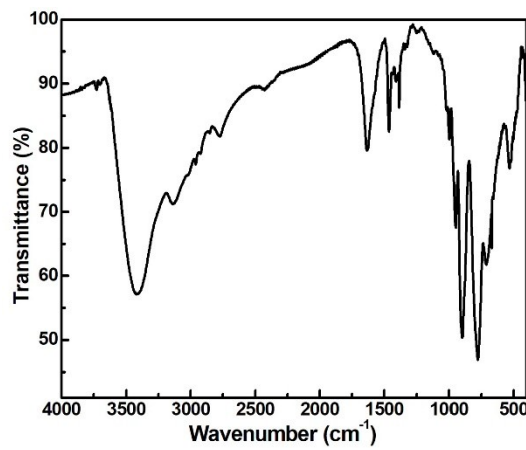


**Figure S6.** The IR spectrum of **1**.

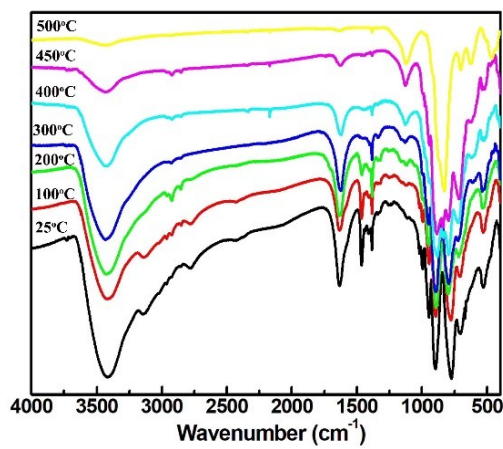


**Figure S7.** The IR spectra of **1** at different temperature.

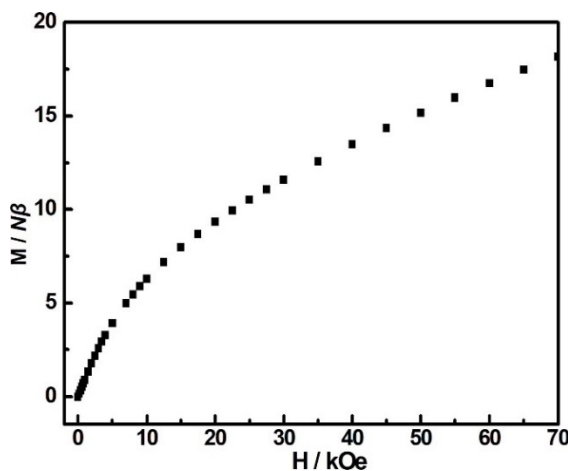


**Figure S8.** Field dependence of the magnetization of **1**.

**Table S1.** Bond valence sum (BVS) calculations of some W, Mn, and Si atoms in **1**.

Atom	BVS	Atom	BVS	Atom	BVS
W1	6.204	W2	6.020	W3	6.158
W4	6.055	W5	6.239	W6	6.187
W7	6.071	W8	6.092	W9	6.091
W10	6.241	W11	6.424	W12	6.157
W13	6.612	W14	6.026	W15	6.038
W16	5.912	W17	6.261	W18	6.300
W19	6.088	W21	6.041	W23	5.875
Mn1	2.564	Mn2	2.384	Mn3	2.197
Si1	4.168	Si2	4.080	Si3	3.945